

https://dspace.org/

Physical layer security over and fading channels

Jules Mouatcho Moualeu; D da Costa; Walaa Hamouda; U Dias; Rausley A.A de Souza

https://hdl.handle.net/10539/28029
ISI

Downloaded from a DSpace repository. https://dspace.org/

Physical Layer Security Over α-κ-μ and α-η-μ Fading Channels

Jules M. Moualeu, *Senior Member, IEEE*, Daniel B. da Costa, *Senior Member, IEEE*, Walaa Hamouda, *Senior Member, IEEE*, Ugo S. Dias, *Senior Member, IEEE*, and Rausley A. A. de Souza, *Member, IEEE*

***Abstract*—In this correspondence, the physical layer security of wireless systems under generalized α-κ-μ and α-η-μ fading with arbitrary fading parameters is analyzed in terms of the secrecy outage probability (SOP). To this end, novel analytical expressions for the lower bound of the SOP are derived. Moreover, an asymptotic secrecy analysis is investigated for each corresponding SOP to get the secrecy diversity gain. Monte Carlo simulations are provided to assess the accuracy of the proposed analytical framework.**

***Index Terms*—α-κ-μ distribution, α-η-μ distribution, PHY security, secrecy capacity.**

I. Introduction

Physical layer (PHY) security has become a promising solution to address the security challenges of wireless networks without relying on traditional encryption techniques. Various works have studied the impact of small-scale fading on the secrecy performance (see [1]–[3] and the references therein). However, the above-mentioned fading models which include Rayleigh, Nakagami-m, Weibull, and Rician, do not cover a variety of fading scenarios experienced in realistic and practical settings. In the past decade, general and flexible fading models such as α-μ, κ-μ and η-μ models have attracted a great deal of interest due to their wide applicability and versatility [4], [5]. Most recently, there have been several research studies devoted to the performance analysis of wireless secure communications over generalized fading distributions in terms of average secrecy capacity, secrecy outage probability (SOP) and probability of strictly positive secrecy capacity (SPSC) (e.g., [6]–[10]).

Inspired by the aforementioned generalized fading models [4], [5], two new generalized fading distributions, i.e., the α-η-μ and the α-κ-μ distributions, that include the α-μ, κ-μ and η-μ models as well as the well-known fading distributions as special cases, have been introduced in [11]. In [12], [13], the performance of wireless communication systems over α-η-μ and α-κ-μ fading channels without considering the security aspect, is analyzed. To the best of the authors' knowledge, there is no reported work in the literature dealing with the secrecy analysis of wireless networks over the α-η-μ or α-κ-μ fading channels. In general, deriving analytical expressions for the performance metrics in PHY security (i.e., ergodic secrecy capacity, SOP and probability of SPSC) when dealing with the α-μ, κ-μ and η-μ fading models is an intricate task, let alone when dealing with more complicated ones such as α-η-μ or α-κ-μ fading channels.

Motivated by the above, the secrecy performance analysis of wireless communication systems over α-η-μ and α-κ-μ fading channels is investigated in this correspondence. Lower bound analytical expressions for the SOP are derived. Although the derived expressions are in the form of infinite series, they converge steadily and rapidly to accurate results after a few terms. Furthermore, asymptotic analyses at high signal-to-noise ratio (SNR) regime are carried out in an effort to obtain the secrecy diversity gain. Finally, some illustrative numerical examples are provided through Monte Carlo simulations to assess the accuracy of the mathematical derivations and insightful discussions are drawn.

The rest of the paper is organized as follows. In Section II, the system and channel models are described. Section III presents the lower bound analysis for the SOP corresponding to both α-η-μ and α-κ-μ fading distributions. The asymptotic studies at high SNR regime for the SOP expressions are provided in Section IV, followed by some representative numerical results and discussions in Section V. Finally, concluding remarks are provided in Section VI.

II. System and Channel Models

Let a three-node classic model where the transmitter Alice (A) sends confidential information to the legitimate receiver Bob (B), while an eavesdropper Eve (E) attempts to intercept or overhears the transmissions through the eavesdropper link. In this context, all the nodes are equipped with a single antenna. It is assumed that both the main channel (Alice-Bob) and eavesdropper channel (Alice-Eve) undergo independent and identically distributed quasi-static generalized fading conditions. Also, both channels experience the same fading type at any given time. In addition, a passive eavesdropping scenario is considered where only the channel state information (CSI) of the main link is known at Alice. In this context, there are two fading conditions under consideration in the above-described setup, i.e., the α-η-μ and α-κ-μ models with arbitrary values of fading parameters.

Manuscript received July 18, 2018; revised November 8, 2018; accepted November 30, 2018. Date of publication December 3, 2018; date of current version January 15, 2019. The work of J. M. Moualeu was supported by the Centre for Telecommunications Access Services (CeTAS) at the University of the Witwatersrand under the Project Code COEF013. The review of this paper was coordinated by Prof. Y. Li. *(Corresponding author: Jules M. Moualeu.)*

J. M. Moualeu is with the School of Electrical and Information Engineering, University of the Witwatersrand, Johannesburg, 2000, South Africa (e-mail: jules.moualeu@wits.ac.za).

D. B. da Costa is with the Department of Computer Engineering, Federal University of Ceará, Sobral 62010-560, Brazil (e-mail: danielbcosta@ieee.org).

W. Hamouda is with the Department of Electrical and Computer Engineering, Concordia University, Montreal, QC H3G 1M8, Canada (e-mail: hamouda@ece.concordia.ca).

U. S. Dias is with the Department of Electrical Engineering, University of Brasília, Brasília 70919-900, Brazil (e-mail: ugodias@ieee.org).

R. A. A. de Souza is with the National Institute of Telecommunications, Santa Rita do Sapucaí 37540-000, Brazil (e-mail: rausley@inatel.br).

Color versions of one or more of the figures in this paper are available online at http://ieeexplore.ieee.org.

Digital Object Identifier 10.1109/TVT.2018.2884832

0018-9545 © 2018 IEEE. Personal use is permitted, but republication/redistribution requires IEEE permission.
See http://www.ieee.org/publications_standards/publications/rights/index.html for more information.

A. The α-η-μ Fading Distribution

The α-η-μ is a general distribution that can be used to model the small-scale variation of the fading signal and includes the Rayleigh, Nakagami-m, Hoyt, one-sided Gaussian, Weibull and η-μ as special cases. Moreover, it captures both the non-linearity and the non-homogeneous nature of the fading channel with no line-of-sight (LOS) component. Using the received signal envelope in [11, Eq. (1)] coupled with a variable transformation, the probability density function (PDF) of the instantaneous SNR γ_i is given by

$$f_{\gamma_i}(x) = \frac{\Psi_i}{\bar{\gamma}_i^{\beta_i}} x^{\beta_i - 1} e^{-\mathcal{A}_i \left(\frac{x}{\bar{\gamma}}\right)^{\tilde{\alpha}_i}} I_{\mu_i - \frac{1}{2}} \left(\zeta_i \left(\frac{x}{\bar{\gamma}_i} \right)^{\tilde{\alpha}_i} \right), \quad (1)$$

in which i denotes B, for legitimate receiver Bob, or E, for eavesdropper Eve, $\beta_i = \tilde{\alpha}_i\,(\mu_i + 1/2)$, $\tilde{\alpha}_i = \alpha_i/2$, $\mathcal{A}_i = \mu_i(1+\eta_i)^2/(2\eta_i)$, $\zeta_i = \mu_i(\eta_i^2 - 1)/(2\eta_i)$, and $\Psi_i = \sqrt{\pi}\tilde{\alpha}_i \mu_i^{\mu_i + \frac{1}{2}} (\eta_i - 1)^{\frac{1}{2} - \mu_i} (\eta_i + 1)^{\frac{1}{2} + \mu_i} / (\eta_i \Gamma(\mu_i))$, $\bar{\gamma}_i$ is the average SNR, $\Gamma(\cdot)$ is the Gamma function and $I_z(\cdot)$ is the modified Bessel function of the first kind [14, Eq. (9.6.20)]. In addition, α_i, η_i and μ_i denote the non-linearity parameter, the ratio between the in-phase and quadrature scattered wave components, and the number of multipath clusters, respectively. With the help of [15, Eq. (8.445)], and after some manipulations, the cumulative distribution function (CDF) of γ_i is given by

$$F_{\gamma_i}(x) = \Xi_i \sum_{n=0}^{\infty} \frac{\left(\frac{\zeta_i}{2}\right)^{2n + \mu_i - 0.5} \Upsilon\left(2n + 2\mu_i, \mathcal{A}_i \left(\frac{x}{\bar{\gamma}_i}\right)^{\tilde{\alpha}_i}\right)}{n!\Gamma(n + \mu_i + 0.5)\mathcal{A}_i^{2(n+\mu_i)}}, \quad (2)$$

where $\Xi_i = \Psi_i/\tilde{\alpha}_i$ and $\Upsilon(\cdot,\cdot)$ is the lower incomplete Gamma function [15, Eq. (8.350.1)].

B. The α-κ-μ Fading Distribution

The α-κ-μ is a general distribution that can be used to represent the small-scale variation of the fading channel with an LOS component. It includes the Rayleigh, Nakagami-m, Rice, Weibull, one-sided Gaussian, and κ-μ distributions as special cases. Using a transformation of variables and [15, Eq. (8.445)] in [11, Eq. (6)], the PDF of the instantaneous SNR γ_i can be written as

$$f_{\gamma_i}(x) = \frac{\tilde{\alpha}_i}{e^{\kappa_i \mu_i}} \sum_{j=0}^{\infty} \frac{\mathcal{B}}{\bar{\gamma}_i^{\tilde{\alpha}_i(\mu_i + j)}} x^{\tilde{\alpha}_i(\mu_i + j) - 1} e^{-\frac{\mu_i(1+\kappa_i)}{\bar{\gamma}_i^{\tilde{\alpha}_i}} x^{\tilde{\alpha}_i}}, \quad (3)$$

where $\mathcal{B} = \mu_i^{\mu_i + 2j} \kappa_i^j (1+\kappa_i)^{\mu_i + j} / (j!\Gamma(\mu_i + j))$ and κ_i is the ratio between the total power of the dominant components and the total power of the scattered waves. Using [15, Eq. (3.381.8)] and after some manipulations, the CDF is given by

$$F_{\gamma_i}(x) = \sum_{l=0}^{\infty} \frac{\mu_i^l \kappa_i^l e^{-\kappa_i \mu_i}}{l!\Gamma(\mu_i + l)} \Upsilon\left(\mu_i + l, \frac{\mu_i(1+\kappa_i)}{\bar{\gamma}_i^{\tilde{\alpha}_i}} x^{\tilde{\alpha}_i}\right). \quad (4)$$

III. SOP Analysis

As mentioned above, a passive eavesdropping scenario is considered here. Such a scenario is applicable to wireless networks where Eve is silent and therefore the corresponding CSI is not known by Alice. In this scenario, an important performance metric used to evaluate the secrecy performance is the SOP. The SOP is defined as the probability that the instantaneous secrecy rate $C_s = \max\{\log_2(1+\gamma_B) - \log_2(1+\gamma_E), 0\}$ [7] falls below a predetermined secrecy transmission rate R_s. Mathematically, the SOP can be formulated as

$$\mathrm{SOP} = \int_0^{\infty} \mathrm{f}_{\gamma_\mathrm{E}}(\gamma_\mathrm{E}) \mathrm{F}_{\gamma_\mathrm{B}}\left(2^{\mathrm{R_s}}(1+\gamma_\mathrm{E}) - 1\right) \mathrm{d}\gamma_\mathrm{E}. \quad (5)$$

However, due to the complicated form of the PDFs and CDFs of the random variable (RV) γ_i for the corresponding generalized fading distributions, it is intractable to obtain an analytical expression for the SOP. Therefore, we resort to deriving the lower bound of the SOP as in [6], such as

$$\mathrm{SOP}^{\mathcal{L}} = \int_0^{\infty} \mathrm{f}_{\gamma_\mathrm{E}}(\gamma_\mathrm{E}) \mathrm{F}_{\gamma_\mathrm{B}}\left(2^{\mathrm{R_s}}\gamma_\mathrm{E}\right) \mathrm{d}\gamma_\mathrm{E}. \quad (6)$$

A. Lower Bound of the SOP Over α-η-μ Channels

Based on (6), the lower bound of the SOP for the α-η-μ scenario can be obtained with the aid of (1) and (2). Therefore, by using [15, Eq. (8.445)] in (1) and plugging (2) into (6), with the aid of [15, Eq. (8.352.6)] and after performing some manipulations, the resulting SOP is given by

$$\mathrm{SOP}^{\mathcal{L}}_{\alpha-\eta-\mu} = \Xi_\mathrm{B} \sum_{\mathrm{n}=0}^{\infty} \frac{\Gamma(2\mathrm{n} + 2\mu_\mathrm{B})(\zeta_\mathrm{B}/2)^{2\mathrm{n}+\mu_\mathrm{B}-0.5}}{\mathrm{n}!\Gamma(\mathrm{n} + \mu_\mathrm{B} + 0.5)\mathcal{A}_\mathrm{B}^{2(\mathrm{n}+\mu_\mathrm{B})}}$$
$$\times \left\{ 1 - \sum_{m=0}^{2n+2\mu_B-1} \sum_{l=0}^{\infty} \frac{2^{m\,\alpha_B\,R_s}\,\mathcal{A}_B^m\,\Psi_E\,(\zeta_E/2)^{2l+\mu_E-0.5}}{m!l!\Gamma(l+\mu_E+0.5)\bar{\gamma}_B^{m\,\tilde{\alpha}_B}\,\bar{\gamma}_E^{\alpha_E\,(l+\mu_E)}} \right.$$
$$\left. \times \int_0^{\infty} \gamma_E^{\omega-1} e^{-\left(\frac{2^{R_s\,\tilde{\alpha}_B}\,A_B}{\bar{\gamma}_B^{\tilde{\alpha}_B}}\gamma_E^{\tilde{\alpha}_B} + \frac{A_E}{\bar{\gamma}_E^{\tilde{\alpha}_E}}\gamma_E^{\tilde{\alpha}_E}\right)} \mathrm{d}\gamma_\mathrm{E} \right\}, \quad (7)$$

where $\omega = \tilde{\alpha}_E(2l + 2\mu_E) + m\tilde{\alpha}_B$. In (7), the integral is of the form $\mathcal{I} = \int_0^{\infty} x^a e^{-(\delta_1 x^p + \delta_2 x^q)} \mathrm{d}x$. In what follows, we evaluate $\mathcal{I}$ in closed-form. With some manipulations, $\mathcal{I}$ can be rewritten as

$$\begin{aligned} \mathcal{I} &= \int_0^{\infty} x^{\frac{a}{p}} e^{-\delta_1 x} e^{-\delta_2 x^{\frac{q}{p}}} \mathrm{d}\left(\mathrm{x}^{\frac{1}{\mathrm{p}}}\right) \\ &= \frac{1}{p} \int_0^{\infty} x^{\frac{a+1}{p}-1} e^{-\delta_1 x} e^{-\delta_2 x^{\frac{q}{p}}} \mathrm{d}x. \end{aligned} \quad (8)$$

From (8), the exponential functions are replaced by their corresponding Meijer G-functions using [16, Eq. (8.4.3.1)] and the resulting integral can be evaluated in closed-form using [17]. After substituting the closed-form expression of $\mathcal{I}$ in (7), the lower bound of the SOP for the α-η-μ fading conditions is given by (9), given at the top of the next page, where $H_{u,v}^{s,t}\left(\cdot \,\middle|\, \begin{matrix} \vdots \\ \vdots \end{matrix}\right)$ is the Fox H-function [16, Eq. (8.3.1.1)]. The Fox H-function has recently become popular in the analysis of the

performance of wireless communications systems, and is not readily available in software computation packages (e.g., MATHEMATICA or MATLAB. However, the work of [18] has proposed an efficient and accurate implementation in MATHEMATICA). Although (9) is expressed in an infinite series form, it converges rapidly and steadily to a precise result after a few terms. To the best of the authors' knowledge, the analytical expression for the lower bound of the SOP is new.

$$\mathrm{SOP}^{\mathcal{L}}_{\alpha-\eta-\mu} = \Xi_{\mathrm{B}} \sum_{\mathrm{n}=0}^{\infty} \frac{\Gamma(2\mathrm{n}+2\mu_{\mathrm{B}})(\zeta_{\mathrm{B}}/2)^{2\mathrm{n}+\mu_{\mathrm{B}}-0.5}}{\mathrm{n}!\Gamma(\mathrm{n}+\mu_{\mathrm{B}}+0.5)\mathcal{A}_{\mathrm{B}}^{2(\mathrm{n}+\mu_{\mathrm{B}})}}$$
$$\left\{ 1 - \frac{1}{\tilde{\alpha}_B} \sum_{m=0}^{2n+2\mu_B-1} \sum_{l=0}^{\infty} \frac{\Psi_E(\zeta_E/2)^{2l+\mu_E-0.5}}{m!l!\Gamma(l+\mu_E+0.5)\bar{\gamma}_E^{\alpha_E(l+\mu_E)}} \right.$$
$$\times \left(\frac{2^{\tilde{\alpha}_B R_s}\mathcal{A}_B}{\bar{\gamma}_B^{\tilde{\alpha}_B}} \right)^{-\frac{\alpha_E(2l+2\mu_E)}{\alpha_B}} H_{1,1}^{1,1}\left(\left(\frac{\mathcal{A}_E}{\bar{\gamma}_E^{\tilde{\alpha}_E}} \right) \left(\frac{2^{\tilde{\alpha}_B R_s}\mathcal{A}_B}{\bar{\gamma}_B^{\tilde{\alpha}_B}} \right)^{-\frac{\alpha_E}{\alpha_B}} \right.$$
$$\left. \left. \left| \begin{matrix} \left(1 - \frac{\alpha_E(2l+2\mu_E)+m\alpha_B}{\alpha_B}, \frac{\alpha_E}{\alpha_B}\right) \\ (0,1) \end{matrix} \right. \right) \right\}. \tag{9}$$

B. Lower Bound of the SOP Over α-κ-μ Channels

Having derived an explicit expression for the lower bound of the SOP over α-η-μ channel, a similar approach can be used to determine an expression for the same performance metric over α-κ-μ channel. To this end, by substituting (3) and (4) into (6), with the aid of [15, Eq. (8.352.6)], [15, Eq. (3.381.11)] and many algebraic manipulations, the lower bound of the SOP is given by

$$\mathrm{SOP}^{\mathcal{L}}_{\alpha-\kappa-\mu} = \sum_{\mathrm{j}=0}^{\infty}\sum_{\mathrm{l}=0}^{\infty} \frac{\tilde{\alpha}_{\mathrm{E}}\mu_{\mathrm{E}}^{\mu_{\mathrm{E}}+2\mathrm{j}}\kappa_{\mathrm{E}}^{\mathrm{j}}(1+\kappa_{\mathrm{E}})^{\mu_{\mathrm{E}}+\mathrm{j}}\mu_{\mathrm{B}}^{\mathrm{l}}\kappa_{\mathrm{B}}^{\mathrm{l}}}{\mathrm{j}!\mathrm{l}!\Gamma(\mu_{\mathrm{E}}+\mathrm{j})\mathrm{e}^{\kappa_{\mathrm{E}}\mu_{\mathrm{E}}}\bar{\gamma}_{\mathrm{E}}^{\tilde{\alpha}_{\mathrm{E}}(\mu_{\mathrm{E}}+\mathrm{j})}}$$
$$\times \left\{ \frac{\Gamma(\mu_E+j)\bar{\gamma}_E^{\tilde{\alpha}_E(\mu_E+j)}}{\tilde{\alpha}_E\left(\mu_E(1+\kappa_E)\right)^{\mu_E+j}} - \sum_{m=0}^{\mu_B+l-1} \frac{\left(\frac{2^{R_s\tilde{\alpha}_B}\mu_B(1+\kappa_B)}{\bar{\gamma}_B^{\tilde{\alpha}_B}}\right)^m}{m!} \right.$$
$$\left. \times \int_0^{\infty} \gamma_E^{\epsilon-1} e^{-\left(\frac{2^{R_s\tilde{\alpha}_B}\mu_B(1+\kappa_B)}{\bar{\gamma}_B^{\tilde{\alpha}_B}}\gamma_E^{\tilde{\alpha}_B} + \frac{\mu_E(1+\kappa_E)}{\bar{\gamma}_E^{\tilde{\alpha}_E}}\gamma_E^{\tilde{\alpha}_E}\right)} \mathrm{d}\gamma_{\mathrm{E}} \right\}, \tag{10}$$

where $\epsilon = \tilde{\alpha}_E(\mu_E+j) + m\tilde{\alpha}_B$. The integral in (10) is given in the same form as $\mathcal{I}$. Using a similar approach used to evaluate $\mathcal{I}$, a closed-form expression of the integral in (10) can be obtained and the resulting expression is substituted into (10) to yield an explicit expression of the lower bound of the SOP in (11).

$$\mathrm{SOP}^{\mathcal{L}}_{\alpha-\kappa-\mu} = \sum_{\mathrm{j}=0}^{\infty}\sum_{\mathrm{l}=0}^{\infty} \frac{\tilde{\alpha}_{\mathrm{E}}\mu_{\mathrm{E}}^{\mu_{\mathrm{E}}+2\mathrm{j}}\kappa_{\mathrm{E}}^{\mathrm{j}}(1+\kappa_{\mathrm{E}})^{\mu_{\mathrm{E}}+\mathrm{j}}\mu_{\mathrm{B}}^{\mathrm{l}}\kappa_{\mathrm{B}}^{\mathrm{l}}}{\mathrm{j}!\mathrm{l}!\Gamma(\mu_{\mathrm{E}}+\mathrm{j})\mathrm{e}^{\kappa_{\mathrm{E}}\mu_{\mathrm{E}}}\bar{\gamma}_{\mathrm{E}}^{\tilde{\alpha}_{\mathrm{E}}(\mu_{\mathrm{E}}+\mathrm{j})}}$$
$$\left\{ \frac{\Gamma(\mu_E+j)\bar{\gamma}_E^{\tilde{\alpha}_E(\mu_E+j)}}{\tilde{\alpha}_E\left(\mu_E(1+\kappa_E)\right)^{\mu_E+j}} - \frac{1}{\tilde{\alpha}_B}\left(\frac{2^{R_s\tilde{\alpha}_B}\mu_B(1+\kappa_B)}{\bar{\gamma}_B^{\tilde{\alpha}_B}}\right)^{-\frac{\alpha_E(\mu_E+j)}{\alpha_B}} \right.$$
$$\left. \times \sum_{m=0}^{\mu_B+l-1} \frac{1}{m!} H_{1,1}^{1,1}\left(\left(\frac{\mathcal{A}_E}{\bar{\gamma}_E^{\tilde{\alpha}_E}}\right) \left(\frac{2^{\tilde{\alpha}_B R_s}\mathcal{A}_B}{\bar{\gamma}_B^{\tilde{\alpha}_B}}\right)^{-\frac{\alpha_E}{\alpha_B}} \right.\right.$$
$$\left.\left. \left| \begin{matrix} \left(1 - \frac{\alpha_E(\mu_E+j)+m\alpha_B}{\alpha_B}, \frac{\alpha_E}{\alpha_B}\right) \\ (0,1) \end{matrix} \right. \right) \right\}. \tag{11}$$

IV. Asymptotic Analysis

In order to get further insights of the role of the various fading parameters in the system performance, an asymptotic analysis will now be carried out by investigating the behavior of the SOP expressions (9) and (11) at high-SNR regime. In what follows, it is assumed that $\bar{\gamma}_B \to \infty$ while $\bar{\gamma}_E$ is fixed, and the aim is to obtain approximate expressions for (9) and (11) in the form $\mathrm{SOP}^{\infty} \approx \mathcal{G}_{\mathrm{c}}\bar{\gamma}^{-\mathcal{G}_{\mathrm{d}}}$, where $\mathcal{G}_c$ and $\mathcal{G}_d$ denote the secrecy array gain and the secrecy diversity gain, respectively. However, for a varying average SNR of the eavesdropper link (i.e., $\bar{\gamma}_E \to \infty$), it can be inferred that secrecy diversity gain is zero due to the high probability of successful eavesdropping.

A. Asymptotic SOP Over α-η-μ Channels

In (2), when $\bar{\gamma}_B \to \infty$, the dominating term is obtained for $n = 0$, which is given by

$$F_{\gamma_B}(\gamma_E) \approx \frac{\Xi_B(\zeta_B/2)^{\mu_B-\frac{1}{2}}}{\Gamma(\mu_B+\frac{1}{2})\mathcal{A}_B^{2\mu_B}} \Upsilon\left(2\mu_B, \frac{\mathcal{A}_B\gamma_E^{\tilde{\alpha}_B}}{\bar{\gamma}_B^{\tilde{\alpha}_B}}\right). \tag{12}$$

Using the following approximation $\Upsilon(s,x) \approx x^s/s$ as $x \to 0$, (12) can be approximated by

$$F_{\gamma_B}(\gamma_E) \approx \frac{\Xi_B\zeta_B^{\mu_B-\frac{1}{2}}\gamma_E^{\alpha_B\mu_B}}{\mu_B 2^{\mu_B+\frac{1}{2}}\Gamma(\mu_B+\frac{1}{2})\bar{\gamma}_B^{\alpha_B\mu_B}}. \tag{13}$$

Using [15, Eq. (8.445] in (1), and the resulting expression together with (13) in (6) and with the aid of [15, Eq. (3.381.11)], the asymptotic SOP is given by

$$\mathrm{SOP}^{\infty}_{\alpha-\eta-\mu} \approx \frac{1}{\bar{\gamma}_{\mathrm{B}}^{\alpha_{\mathrm{B}}\mu_{\mathrm{B}}}} \left\{ \frac{\Psi_{\mathrm{E}}\Xi_{\mathrm{B}}\zeta_{\mathrm{B}}^{\mu_{\mathrm{B}}-\frac{1}{2}}2^{\mathrm{R_s}\alpha_{\mathrm{B}}\mu_{\mathrm{B}}}}{\mu_{\mathrm{B}}2^{\mu_{\mathrm{B}}+\frac{1}{2}}\Gamma\left(\mu_{\mathrm{B}}+\frac{1}{2}\right)} \right.$$
$$\times \sum_{l=0}^{\infty} \frac{(\zeta_E/2)^{2l+\mu_E-0.5}}{l!\Gamma(2l+\mu_E+0.5)} \Gamma\left(2(l+\mu_E)+2\frac{\alpha_B}{\alpha_E}\mu_B\right)$$
$$\left. \times \frac{\bar{\gamma}_E^{\alpha_B\mu_B}}{\tilde{\alpha}_E\mathcal{A}_E^{2(l+\mu_E)+\frac{\alpha_B}{\alpha_E}\mu_B}} \right\}. \tag{14}$$

From the above expression, it is evident that the secrecy diversity gain is given by $\mathcal{G}_d = \alpha_B\mu_B$ which provides useful insights on the fading parameters on the system performance.

B. Asymptotic SOP Over α-κ-μ Channels

In order to approximate (4) as $\bar{\gamma}_B \to \infty$, it is noted that the dominating term corresponds to $j = 0$. Using $\Upsilon(s,x) \approx x^s/s$ as $x \to 0$,

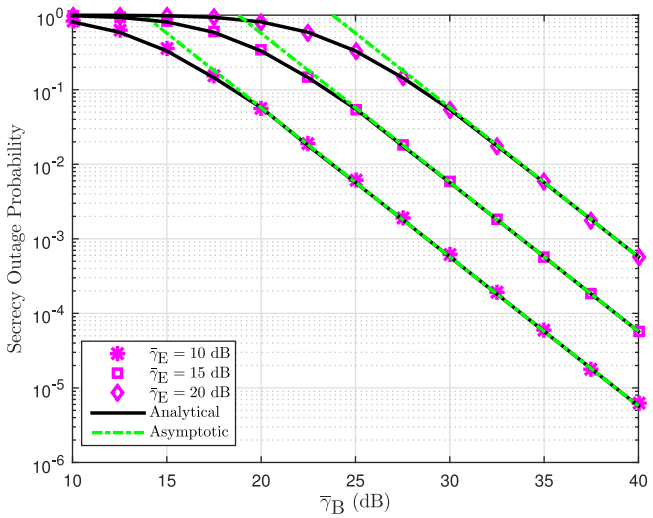


Fig. 1. Lower bound of the SOP versus average SNR $\bar{\gamma}_B$ for $\alpha_B = 4$, $\eta_B = 1.6$, $\mu_B = 0.5$, $\alpha_E = 2$, $\eta_E = 2.5$, $\mu_E = 1.5$, $R_s = 1$ bits/s/Hz, and various $\bar{\gamma}_E$. The markers represent Monte Carlo simulations.

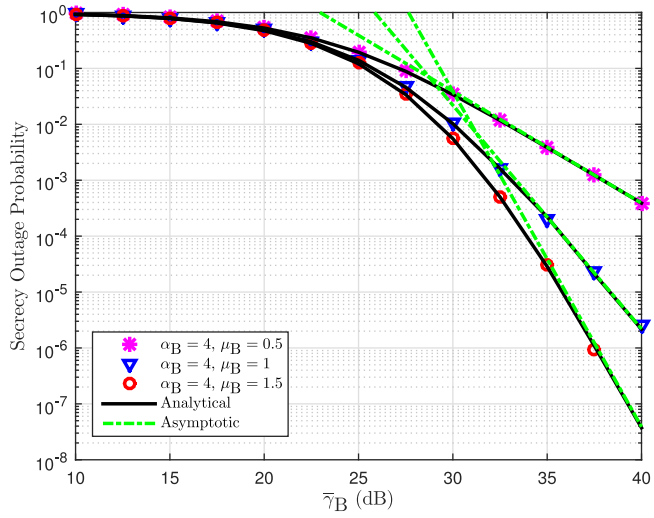


Fig. 2. Lower bound of the SOP versus average SNR $\bar{\gamma}_B$ for $\alpha_E = 2$, $\eta_E = 0.5$, $\mu_E = 0.5$, $\eta_B = 3$, $\bar{\gamma}_E = 15$ dB, and $R_s = 2$ bits/s/Hz. The markers represent Monte Carlo simulations.

(4) is approximated by

$$F_{\gamma_B}(\gamma_E) \approx \frac{\mu_B^{\mu_B - 1}(1+\kappa_B)^{\mu_B}\gamma_E^{\tilde{\alpha}_E \mu_B}}{\Gamma(\mu_B) e^{\kappa_B \mu_B}\bar{\gamma}_B^{\tilde{\alpha}_B \mu_B}}. \tag{15}$$

By substituting (3) and (15) in (6), and with the help of [15, Eq. (3.381.11)] and some algebraic manipulations, the asymptotic SOP is given by

$$\mathrm{SOP}^{\infty}_{\alpha-\kappa-\mu} \approx \frac{1}{\bar{\gamma}_{\mathrm{B}}^{\tilde{\alpha}_{\mathrm{B}}\mu_{\mathrm{B}}}} \left\{ \sum_{\mathrm{j}=0}^{\infty} \frac{2^{\mathrm{R_s}\tilde{\alpha}_{\mathrm{B}}\mu_{\mathrm{B}}}\mu_{\mathrm{B}}^{\mu_{\mathrm{B}}-1}\kappa_{\mathrm{E}}^{\mathrm{j}}}{\mathrm{j}!\Gamma(\mu_{\mathrm{B}})\Gamma(\mu_{\mathrm{E}}+\mathrm{j})\mu_{\mathrm{E}}^{\mathrm{j}+\frac{\alpha_{\mathrm{B}}}{\alpha_{\mathrm{E}}}\mu_{\mathrm{B}}}} \right.$$

$$\left. \times \frac{(1+\kappa_B)^{\mu_B}\bar{\gamma}_E^{\tilde{\alpha}_B\mu_B}}{(1+\kappa_E)^{\frac{\alpha_B}{\alpha_E}\mu_B} e^{\kappa_E\mu_E+\kappa_B\mu_B}} \Gamma\left(\mu_E + j + \frac{\alpha_B}{\alpha_E}\mu_B\right) \right\}. \tag{16}$$

The above expression shows that the secrecy diversity gain is given by $\mathcal{G}_d = \tilde{\alpha}_B \mu_B$, where $\tilde{\alpha}_B = \alpha_B/2$, and is independent of κ_B. To the best of the authors' knowledge, the analytical expressions derived in (14) and (16) have not been previously reported in the existing literature.

V. Numerical Results and Discussions

In this section, some representative numerical examples are provided along with Monte Carlo simulations to verify the accuracy of the proposed mathematical derivations and to illustrate the effects of the channel parameters $\alpha_i, \eta_i, \kappa_i$, and μ_i. Although the derived analytical expressions for the SOP in (9) and (11) include infinite series, this is not an issue since such series rapidly and steadily converge after a few terms to achieve a sufficient level of accuracy. In particular, fairly precise results can be obtained after truncating the series into 8 terms.

In Fig. 1, the performance of the SOP for the α-η-μ conditions versus the average main link SNR $\bar{\gamma}_B$ for various values of $\bar{\gamma}_E$ is illustrated. For some fading parameters of the main and eavesdropper links, as the average SNR of the eavesdropper link increases, the SOP increases. This makes sense because an increasing $\bar{\gamma}_E$ (leading to a high probability of successful eavesdropping) is detrimental to the secrecy performance; in this case, the SOP performance degrades regardless of the average SNR of the main link $\bar{\gamma}_B$. In addition, it is seen that the lower bound of the SOP closely matches the simulated results over the entire SNR regime, confirming that derived lower bound of the SOP is a tight approximation of the exact which could not be obtained because of the intricacy of the analytical expressions associated with the aforementioned generalized fading distributions.

Fig. 2 shows the lower bound of the SOP versus $\bar{\gamma}_B$ for various fading parameters assuming α-η-μ fading. It can be noticed, hereinafter, that there is a very good agreement between the proposed analytical framework (lower bound of the SOP) and the Monte Carlo simulations (markers). Additionally, it can be observed that the asymptotic curves accurately approximate the lower bound curves at high-SNR regime. As the curves have different slopes, this corroborates the proposed asymptotic analysis which shows that under this fading condition, the secrecy diversity gain is dependent of the fading parameters α_B and μ_B. Note that the diversity gain equals to $\mathcal{G}_d = \alpha_B \mu_B$, which can be confirmed by the slope of the curves. Unlike in Fig. 1 where the curves have the same slope ($\alpha_B = 4$ and $\mu_B = 0.5$ in all cases), Fig. 2 depicts some curves with different slopes.

Both Fig. 3 and Fig. 4 show the SOP performance versus $\bar{\gamma}_B$ under the α-κ-μ fading conditions. First, the SOP performance for some fading parameters and various values of the secrecy target rate R_s, is depicted in Fig. 3. It is evident that a decreasing target rate leads to an improvement of the secrecy performance in the context of the SOP. In addition, the slopes of the curves are identical since the fading parameters of the main link are fixed here, hence the same secrecy diversity gain is achieved. In Fig. 4, it is noted that different diversity orders are

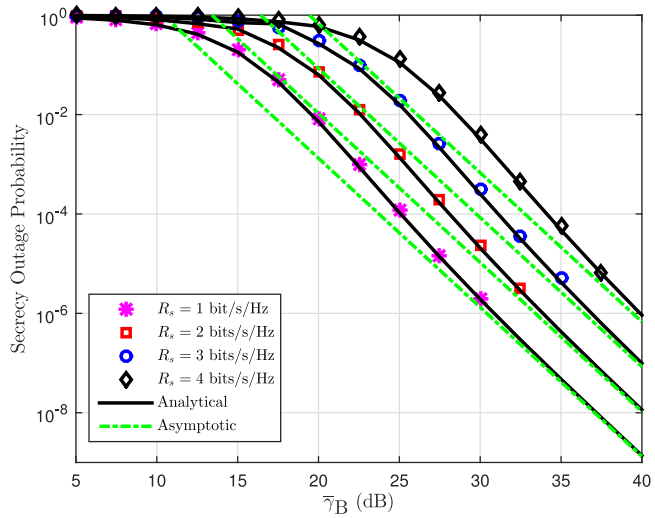


Fig. 3. Lower bound of the SOP versus average SNR $\bar{\gamma}_B$ for $\alpha_B = 2$, $\kappa_B = 2.5$, $\mu_B = 3$, $\alpha_E = 4$, $\kappa_E = 0.5$, $\mu_E = 0.5$, and $\bar{\gamma}_E = 10$ dB. The markers represent Monte Carlo simulations.

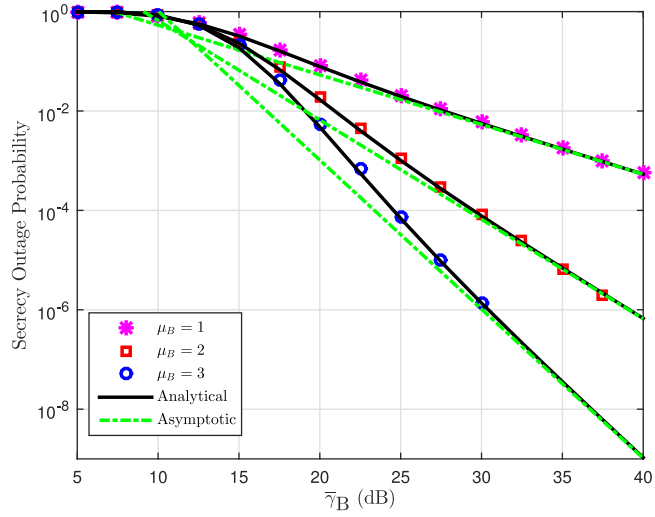


Fig. 4. Lower bound of the SOP versus average SNR $\bar{\gamma}_B$ for $\alpha_B = 2$, $\kappa_B = 2.5$, $\alpha_E = 4$, $\kappa_E = 0.5$, $\mu_E = 1.5$, $R_s = 1$ bit/s/Hz, and $\bar{\gamma}_E = 10$ dB. The markers represent Monte Carlo simulations.

obtained for different fading parameters of the main links and in all cases $\mathcal{G}_d = \frac{\alpha_B \mu_B}{2}$ is corroborated, confirming the proposed asymptotic analysis. Furthermore, it is evident that the asymptotic curves tightly approximate the lower bound of the SOP as well as the Monte Carlo simulations in the high-SNR regimes.

VI. Conclusion

This work addressed the secrecy performance of wireless communications systems over the new generalized α-η-μ and α-κ-μ fading channels. Novel analytical expressions were derived for the lower bound of the SOP and were validated through Monte Carlo simulations. The derived analytical expressions for the SOP closely matched the exact SOP. Moreover, an asymptotic analysis for the SOP was carried out and revealed to be in perfect agreement with the lower bound of the SOP at high SNR. It was shown that the secrecy performance highly depends on the fading parameters, especially of the main links in the high-SNR regime.

References

[1] M. Kamel, W. Hamouda, and A. Youssef, "Physical layer security in ultra-dense networks," *IEEE Wireless Commun. Lett.*, vol. 6, no. 5, pp. 690–693, Oct. 2017.

[2] X. Liu, "Probability of strictly positive secrecy capacity of the Rician–Rician fading channel," *IEEE Wireless Commun. Lett.*, vol. 2, no. 1, pp. 50–53, Feb. 2013.

[3] H. Lei *et al.*, "Secrecy outage performance of transmit antenna selection for MIMO underlay cognitive radio systems over Nakagami-m channels," *IEEE Trans. Veh. Technol.*, vol. 66, no. 3, pp. 2237–2250, Mar. 2017.

[4] M. D. Yacoub, "The α-μ distribution: A physical fading model for the Stacy distribution," *IEEE Trans. Veh. Technol.*, vol. 56, no. 1, pp. 27–34, Jan. 2007.

[5] M. D. Yacoub, "The η-μ distribution and the κ-μ distribution," *IEEE Antennas Propag. Mag.*, vol. 49, no. 1, pp. 68–81, Feb. 2007.

[6] N. Bhargav, S. L. Cotton, and D. E. Simmons, "Secrecy capacity analysis over κ-μ fading channels: Theory and applications," *IEEE Trans. Commun.*, vol. 64, no. 7, pp. 3011–3024, Jul. 2016.

[7] H. Lei, I. S. Ansari, G. Pan, B. Alomair, and M. S. Alouini, "Secrecy capacity analysis over α-μ fading channels," *IEEE Commun. Lett.*, vol. 21, no. 6, pp. 1445–1448, Jun. 2017.

[8] J. M. Moualeu and W. Hamouda, "On the secrecy performance analysis of SIMO systems over κ-μ fading channels," *IEEE Commun. Lett.*, vol. 21, no. 11, pp. 2544–2547, Nov. 2017.

[9] J. M. Moualeu and W. Hamouda, "Secrecy performance analysis over mixed α-μ and κ-μ fading channels," in *Proc. IEEE Wireless Commun. Netw. Conf.*, Barcelona, Spain, Apr. 2018, pp. 1–6.

[10] M. Srinivasan and S. Kalyani, "Secrecy capacity of κ-μ shadowed fading channels," *IEEE Commun. Lett.*, vol. 22, no. 8, pp. 1728–1731, Aug. 2018.

[11] G. Fraidenraich and M. D. Yacoub, "The α-η-μ and α-κ-μ fading distributions," in *Proc. IEEE 9th Int. Symp. Spread Spectr. Techn. Appl., Manaus-Amazon, Brazil*, Apr. 2006, pp. 16–20.

[12] E. Salahat and A. Hakam, "Performance analysis of α-η-μ and α-κ-μ generalized mobile fading channels," in *Proc. 20th Eur. Wireless Conf.*, Berlin, Germany, Apr. 2014, pp. 16–20.

[13] O. S. Badarneh and M. S. Aloqlah, "Performance analysis of digital communication systems over α-η-μ fading channels," *IEEE Trans. Veh. Technol.*, vol. 65, no. 10, pp. 7972–7281, Oct. 2016.

[14] M. Abramowitz and I. A. Stegun, *Handbook of Mathematical Functions with Formulas, Graphs, and Mathematical Tables*. New York, NY, USA: Dover, 1972.

[15] I. S. Gradshteyn and I. M. Ryzhik, *Table of Integrals, Series, and Products*, 7th ed. San Diego, CA, USA: Academic, 2007.

[16] A. P. Prudnikov, Y. A. Brychkov, and O. I. Marichev, *Integrals and Series, Vol. 3: More Special Functions*. New York, NY, USA: Oxford Univ. Press, 1990.

[17] Wolfram Research Meijer G-Function. [Online]. Available: http://functions.wolfram.com/07.34.21.0012.01

[18] F. Yilmaz and M.-S. Alouini, "Product of the powers of generalized Nakagami-m variates and performance of cascaded fading channels," in *Proc. IEEE Global Telecommun. Conf.*, Honolulu, HI, USA, 2009, pp. 1–8.